PCCP

Accepted Manuscript

ROYAL SOCIETY OF CHEMISTRY

www.rsc.org/pccp

Disulfuric acid dissociated by two water molecules: Ab initio and density functional theory calculations

Seong Kyu Kim,[1,*] Han Myoung Lee,[2] Kwang S. Kim[2,*]

[1]*Department of Chemistry, Sungkyunkwan University, Suwon 440-746, Korea*

[2]*Center for Superfunctional Materials, Department of Chemistry, Ulsan Institute of Science and Technology (UNIST), Ulsan 689-798, Korea*

*Corresponding authors, skkim@skku.edu, kimks@unist.ac.kr

Abstract

We have studied geometries, energies and vibrational spectra of disulfuric acid ($H_2S_2O_7$) and its anion ($HS_2O_7^-$) hydrated by a few water molecules, using density functional theory (M062X) and ab initio theory (SCS-MP2 and CCSD(T)). The most noteworthy result is found in $H_2S_2O_7(H_2O)_2$ in which the lowest energy conformer shows deprotonated $H_2S_2O_7$. Thus, $H_2S_2O_7$ requires only two water molecules, the fewest number of water molecules for deprotonation among various hydrated monomeric acids reported so far. Even the second deprotonation of the first deprotonated species $HS_2O_7^-$ needs only four water molecules. The deprotonation is supported by vibration spectra, in which acid O-H stretching peaks disappear and specific three O-H stretching peaks for H_3O^+ (eigen structure) appear. We also have kept track of variations in several geometrical parameters, atomic charges, hybrid orbital characters upon addition of water. As the number of water molecules added increases, the S-O bond weakens in the case of $H_2S_2O_7$, but strengthens in the case of $HS_2O_7^-$. It implies that the decomposition leading to H_2SO_4 and SO_3 hardly occurs prior to the 2nd deprotonation at low temperatures.

1. Introduction

Hydrated clusters of solutes may provide essential information for understanding solvation phenomena of molecular systems.[1] The dissociation and deprotonation phenomena of solute molecules are highly complicated phenomena. As such, a number of studies have been reported on diverse cations,[2-6] anions,[7-8] acids,[9-22] bases,[23-24] salts[25-27] as well as aromatic and bio molecules[28-31] hydrated by various numbers of water molecules. In particular, hydration of acids is of importance in aerosol nucleation process in atmosphere.[32]

When the solute is a strong Brönsted-Lowry acid, the O-H bond becomes more polarized by hydration, and the deprotonation of the acid can be induced if the number of water molecules exceeds a certain limit. The least number of water molecules to induce deprotonation is expected to be related to acid strength. For example, the deprotonation of strong acids HCl, HBr or HI needs at least four water molecules,[33-34] while that of HF requires many water molecules.[35-37] The deprotonation of H_2SO_4 is possible with three or four water molecules.[17,38-40] The deprotonation of $HClO_4$ is possible with three water molecules.[41] Meanwhile, the H_2SO_4 dimer, though it is not a single molecule, was considered to be dissociable with two water molecules.[18]

There are many more acids that are stronger than the above acids. They are classified as 'superacid'. However, detailed studies on most superacids have been limited because of their general instability. Several molecules in sulfur oxoacids family are expected to be superacid according to ab initio calculations.[42-43] Among them, we focus here on disulfuric acid (or pyrosulfuric acid, $H_2S_2O_7$), which is a useful intermediate in numerous industrial processes.

When sulfur trioxide is mixed with anhydrous sulfuric acid, a solution of fuming sulfuric acid or so-called oleum is formed. Disulfuric acid is a major constituent of oleum as it is formed via equilibrium:

$$SO_3 + H_2SO_4 \leftrightarrows H_2S_2O_7 \qquad (1)$$

Oleum is a useful chemical agent for numerous industrial applications. For example, it can be used as a safe intermediate for transporting sulfuric acid since certain compositions of oleum are solid at room temperature. Sulfuric acid can be regenerated by reacting disulfuric acid in oleum with water:

$$H_2S_2O_7 + H_2O \leftrightarrows 2H_2SO_4 \qquad (2)$$

Disulfuric acid is known as a solid with the melting temperature of 36 ^oC according to National Institute of Standards and Technology (NIST) reference data base.[44] This information is widely available in numerous encyclopedia and internet sites such as wiki, pubchem, and chemfinder. However, pure disulfuric acid has never been isolated. The reference data are based on the work of Waytt and coworkers in 1950's, in which mixtures of anhydrous sulfuric acid with varying amounts of SO_3 were prepared in cryoscopic condition and their freezing points were measured.[45-46] They assumed that the mixture is dominated by $H_2S_2O_7$ when the mole fraction of SO_3 is 0.5. This assumption is plausible since the forward reaction of (2) is highly exothermic.

However, the simple picture of the three component equilibrium in oleum may be complicated if other species are present in the mixture. Ionized species such as HSO_4^- and $HS_2O_7^-$ may exist since H_2SO_4 and $H_2S_2O_7$ are strong acids. Presence of higher polysulfuric acids such as $H_2S_3O_{10}$ or polymeric sulfur trioxide such as S_3O_9 under certain conditions has been suggested in several Raman[47-49] and IR works.[49-51]

The theoretical investigations on disulfuric acid have been scarce. The first ab initio calculation for $H_2S_2O_7$ and its anion appeared in the work of Otto and Steudel,[42] and followed by Abedi et al.[43,52] However, the primary purposes of their works were to evaluate the acidity in the sulfur oxoacid family,[42,43] or the dissociation[52] of sulfur oxoanions, and therefore the analyses were not focused on disulfuric acid.

In this paper, we present ab initio and density functional theory (DFT) results of water clusters of $H_2S_2O_7$ and its anion. Changes of geometrical parameters, atomic charges, bond orders, vibrational frequencies as well as thermodynamic functions are monitored as the number of water molecules is changed. The information is used to

find deprotonation trend in their water clusters. We wish to know how the deprotonation competes with the decomposition $H_2S_2O_7 \rightarrow H_2SO_4 + SO_3$, which is a crucial step in equilibrium reaction (1).

2. Methods

Before performing DFT and ab initio calculations, diverse geometries of each cluster were guessed based on known structures of acid-water and water-water clusters. These various geometries were screen-tested using a molecular mechanical force field or a semiempirical parametrized Hamiltonian in Spartan' 14 program.[53] In this way, 20 – 50 geometries for the cluster of each size were obtained and used as starting geometries for optimization by using a hybrid functional M062X[54] with TZVP basis set.[55] From here on, this method is referred to M062X/TZVP or further to M062X. The low-lying energy structures were further optimized using the spin-component scaled (SCS) [56] second order Möller-Plesset perturbation (MP2) theory implemented by resolution of identity (RI) method[57] with aug-cc-pVTZ basis set. From here on, this method is referred to SCS-MP2/aVTZ. For $H_2S_2O_7(H_2O)_{0\text{-}2}$ clusters, single point calculations using the SCS-MP2 method with aug-cc-pVQZ basis set or the CCSD(T) method with aug-cc-pVTZ basis set were carried out to obtain more accurate binding energies;[58] they are referred to SCS-MP2/aVQZ and CCSD(T)/aVTZ, respectively. In the SCS-MP2 and the CCSD(T) calculations, consistent auxiliary basis set was added for the valence electrons while the basis set for the core electrons was frozen.

For the selected low energy conformers, vibrational frequencies were obtained using the M062X method to provide the zero point energy (ZPE) and the thermal energy corrections to give Gibbs free energy G_T at temperature T. Natural bond order (NBO) analyses[59] for the SCS-MP2 results were carried out to find the atomic charges, orbital populations. We also report Wiberg bond orders[60] from the NBO analyses, even though interpreting their values for nonbonding interactions needs a caution.

We used the Gaussian 09 program[61] for the M062X calculations and the Turbomole V6.4 program[62] for the RI-MP2 and the RI-CCSD(T) calculations.

3. Results

3-1. Geometries of $H_2S_2O_7$ and $HS_2O_7^-$

The final optimized geometries for $H_2S_2O_7$ and HSO_7^- are shown in Figure 1. The selected values for the optimized geometrical parameters and the energies are summarized in Table 1.

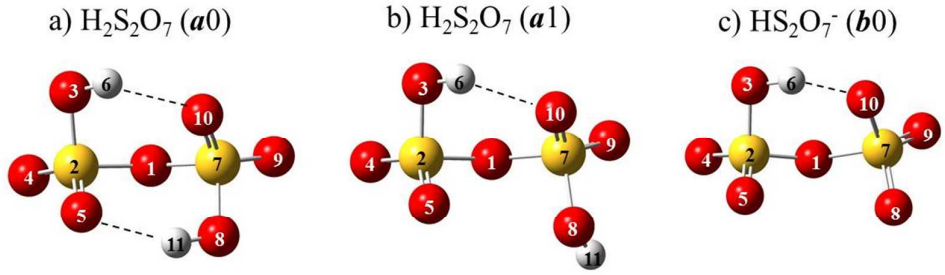

Figure 1. Geometries of $H_2S_2O_7$ (a and b) and $HS_2O_7^-$ (c) at the SCS-MP2/aVTZ level. For the $H_2S_2O_7$, ***a***0 is the geometry of the global minimum and ***a***1 is that of the next lowest energy. Weak intramolecular H-bonds are shown with the broken straight lines.

First, we wish to make a convention for numbering atoms. For $H_2S_2O_7$, hydrogen No. 6 shows a higher tendency of intramolecular H-bonding, while hydrogen No. 11 prefers to either form a H-bond intermolecularly or undergo dissociation upon clustering with water molecules. This convention is maintained in numbering atoms of $HS_2O_7^-$. Second, the convention to distinguish conformers is required; we use ***a***w_nN (or ***b***w_nN) notations, where ***a*** and ***b*** indicate $H_2S_2O_7$ and $HS_2O_7^-$, respectively. n is the number of water molecules and N is the ascending order of the conformer energy for the cluster of given size; N=0 for the global minimum energy conformer; N=1 for the next lowest energy conformer, etc. We also mention here that by the 'energy' of conformer we mean the electronic energy (E_e) given by the SCS-MP2/aVTZ calculation plus ZPE given by the M062X/TZVP calculation, unless stated otherwise.

Table 1. Selected geometrical parameters, bond orders, and energy values for the optimized $H_2S_2O_7$ and $HS_2O_7^-$.[a]

	$H_2S_2O_7$		$HS_2O_7^-$
	***a*0**	***a*1**	***b*0**
bond length (Å)			
O10-H6	1.989	2.038	1.678
O1-S2	1.653	1.675	1.586
O1-S7	1.653	1.627	1.780
bond order[b]			
O10-H6	0.013	0.002	0.060
O1-S2	0.666	0.704	0.784
O1-S7	0.666	0.617	0.485
S7-O8	0.835	0.825	1.264
angle (degree)			
O1-S7-O8-H11	-60.2	81.4	-
δE (kcal/mol)			
δE_e	0	3.15	-
δE_0	0	3.30	-
δG_{100K}	0	2.72	-

[a]All the values were obtained at the SCS-MP2/aVTZ level. $\delta E_e/\delta E_0$ is the relative ZPE-uncorrected/corrected energy and $\delta G_{100\,K}$ is the relative Gibbs free energy at 100 K, where the ZPE and thermal energy used the M062X/TZVP values. [b]Wiberg bond order.

The geometry of the global minimum (***a*0**) of $H_2S_2O_7$ shows a C_2 symmetry, where each of the two hydrogens is weakly H-bonded intramolecularly to an oxygen atom across the S2-O1-S7 frame. This picture is consistent with the reports by Otto and Steudel[42] or by Abedi and Farrokhpour.[43] Each of the two O-H bonds and the two O-S bonds can be twisted to give several local minimum geometries. Energies of those conformers but the next lowest one (***a*1**) are found to be higher by at least 4 kcal/mol, and thus are not reported here. In the next lowest energy conformer, the intramolecular H-bonding is lifted from one (H11) of the two hydrogens while it is maintained in the other hydrogen (H6). The energy of this conformer is 3.30 kcal/mol higher than that of the global minimum.

The geometrical parameters of $HS_2O_7^-$ are very similar to those in Otto and Steudel's work[42] and in X-ray crystalline data.[63] The sole hydrogen (H6) is H-bonded intramolecularly to an oxygen atom (O10) across the S2-O1-S7 frame. This intramolecular H-bonding is much stronger than that of $H_2S_2O_7$; the H6-O10 distance

decreases from 1.989 Å to 1.678 Å. The strengthened intramolecular H-bonding must increase the energy barrier of the O-H twisting. As the result, we found only one conformer (***b***0). The other noteworthy geometrical parameters are related to the weakened O1-S7 bond in the anion. Upon the deprotonation, the O1-S7 bond lengthens from 1.653 Å to 1.780 Å and the bond order decreases from 0.666 to 0.485. On the contrary, the O1-S2 bond strengthens in the anion. This unbalance of the two O-S bonds in the anion implies a tendency for O1-S7 dissociation to produce SO_3. Whether the dissociation/deprotonation tendency increases or decreases upon clustering with water has been one of our concerns in the calculation.

3-2. Geometries of $H_2S_2O_7(H_2O)_{1-3}$

Geometries of $H_2S_2O_7(H_2O)_{1-3}$ conformers, optimized at the SCS-MP2/aVTZ level, are shown in Figure 2. Their binding energies are written in Table 2. Only those conformers whose energy is higher by less than 3.0 kcal/mol than the global minimum in the cluster of corresponding size are reported. For $H_2S_2O_7(H_2O)_{1-2}$ conformers, the binding energies obtained from the single point calculation with SCS-MP2/aVQZ and CCSD(T)/aVTZ are also listed. The complete basis set (CBS) limit value for SCS-MP2 was estimated by extrapolating the aVTZ and aVQZ results,[64,65] while that of CCSD(T) method was obtained by adding the CBS correction term at the MP2/aVTZ and MP2/aVQZ levels to the CCSD(T)/aVTZ energy.[66] The values of ΔG_{100K} as well as ΔE are also listed.

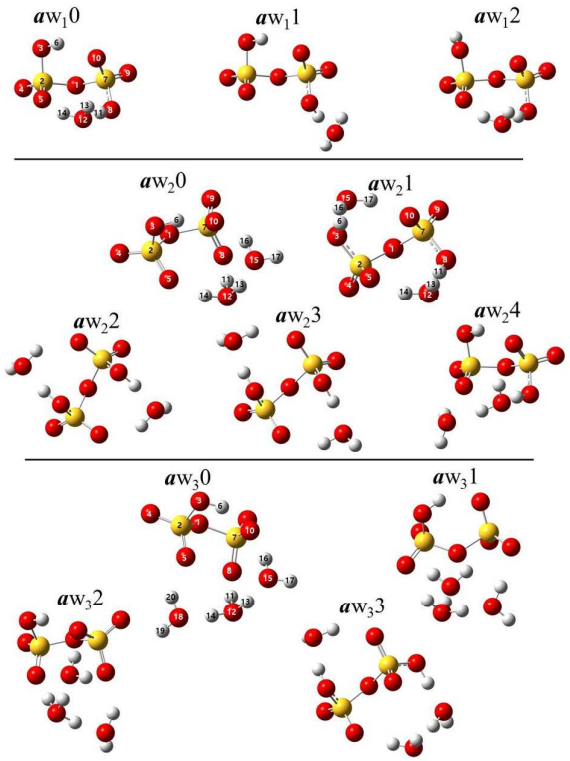

Figure 2. Geometries of $H_2S_2O_7(H_2O)_{1\text{-}3}$ low energy conformers, optimized at the RI-MP2/aVTZ level.

In the lowest energy conformer of $H_2S_2O_7(H_2O)_1$ or ***a***w$_1$0, an intramolecular H-bonding (O5-H11) is lifted to make an intermolecular H-bonding with a water while the other hydrogen (H6) maintains the intramolecular H-bonding nature. The geometry of the acid moiety of this conformer is similar to that of ***a***1 in the directions of the two O-H's. As the energy of ***a***w$_1$0 is 2.63 kcal/mol less than any other conformers, it must be dominant in the cluster of this size at low temperatures.

For $H_2S_2O_7(H_2O)_2$, the lowest energy structure is ***a***w$_2$0, followed by ***a***w$_2$1 and ***a***w$_2$2. The lowest energy conformer ***a***w$_2$0 has deprotonated geometry. The ZPE corrected (uncorrected) binding energy ($\Delta E_0/\Delta E_e$) of ***a***w$_2$0 is lower than ***a***w$_2$1 by 0.2 (1.2), 0.3 (1.2), 0.3 (1.2), 0.04 (1.1), and 0.2 (1.3) kcal/mol at the SCS-MP2/aVTZ, SCS-MP2/aVQZ, SCS-MP2/CBS, CCSD(T)/aVTZ, and CCSD(T)/CBS levels,

respectively. At 100 K, the binding free energy ($-\Delta G_{100}$) at 100 K for ***a***w$_2$0 is 0.1 kcal/mol lower than ***a***w$_2$1 at the CCSD(T)/CBS level, and ***a***w$_2$0 remains to be the most stable up to ~150 K. The sums of NBO charges of H_3O^+ and $HS_2O_7^-$ moieties of ***a***w$_2$0 are +0.820 and -0.869, respectively, indicating the formation of near cationic and near anionic species. The other $H_2S_2O_7(H_2O)_2$ conformers show no deprotonated geometry. In the deprotonated conformer, the two water molecules bind H on the same side of $H_2S_2O_7$ and form an effective H-bonding network forming strong H-bond interactions charged by deprotonated H^+, while in the un-deprotonated conformers, the two water molecules bind on the different side of $H_2S_2O_7$.

For $H_2S_2O_7(H_2O)_3$, three conformers, ***a***w$_3$0, ***a***w$_3$1 and ***a***w$_3$2 have nearly the same energy within 1.0 kcal/mol. They all show the deprotonated geometries as three H_2O molecules bind on the same side of $H_2S_2O_7$ and form an effective H-bonding network. The $HS_2O_7^-$ and H_3O^+ moieties become more negative and positive as one more water molecule is added to $H_2S_2O_7(H_2O)_2$. In contrast, ***a***w$_3$3 shows no deprotonated geometry as one water molecule and the other two water molecules bind on the other side of $H_2S_2O_7$. The energy of this un-deprotonated conformer is fairly high, 2.51 kcal/mol higher than the global minimum.

Table 2. Internal binding energies and Gibbs free energy changes (kcal/mol) of low energy conformers of $H_2S_2O_7(H_2O)_{1-3}$.[a]

	SCS-MP2				CCSD(T)		
	aVTZ		aVQZ	CBS[b]	aVTZ	CBS[c]	
	$-\Delta E_e(-\Delta E_0)$	$-\Delta G_{100K}$	$-\Delta E_e$	$-\Delta E_e$	$-\Delta E_e$	$-\Delta E_e(-\Delta E_0)$	$-\Delta G_{100K}$
$H_2S_2O_7(H_2O)_1$							
aw$_1$0	12.9(11.1)	8.7	12.6	12.5	14.0	13.7(11.8)	9.4
aw$_1$1	10.1(8.4)	6.3	9.9	9.8	10.7	10.4(8.8)	6.6
aw$_1$2	10.0(8.2)	5.9	9.8	9.6	10.6	10.2(8.4)	6.0
$H_2S_2O_7(H_2O)_2$							
aw$_2$0[d]	25.4(20.8)	15.8	25.0	24.8	27.4	26.9(22.3)	17.3
aw$_2$1[e]	24.2(20.6)	15.7	23.7	23.4	26.3	25.6(22.1)	17.2
aw$_2$2[e]	24.0(20.3)	15.4	23.4	22.9	26.1	25.2(21.5)	16.6
aw$_2$3[e]	23.3(19.5)	14.5	22.7	22.3	25.4	24.5(20.7)	15.7
aw$_2$4	23.0(19.1)	14.2	22.6	22.3	25.0	24.4(20.5)	15.6
$H_2S_2O_7(H_2O)_3$							
aw$_3$0[d]	38.0(30.8)	23.3					
aw$_3$1[d]	37.0(29.9)	22.2					
aw$_3$2[d]	37.2(29.8)	22.2					
aw$_3$3	35.6(28.3)	22.4					

[a] ΔE_e is the difference in electronic energy (E_e) between the cluster and the individual molecules, while ΔE_0 is the difference in ZPE-corrected energies (E_0). No correction for basis set superposition error was made because of the dissociation phenomena. The ZPE and the thermal correction for ΔG_{100K} used the M062X/TZVP values.

[b] $E^{SCS\text{-}MP2/CBS} = (4^3 E^{SCS\text{-}MP2/aVQZ} - 3^3 E^{SCS\text{-}MP2/aVTZ})/(4^3\text{-}3^3)$

[c] $E^{CCSD(T)/CBS} = E^{CCSD(T)/aVTZ} + (E^{MP2/CBS} - E^{MP2/aVTZ})$. Here, we used MP2 values instead of SCS-MP2 values, while both cases give almost the same CBS values within 0.1 kcal/mol. [d] deprotonated geometry, [e] C_2 symmetry.

3-3. Geometries of $[HS_2O_7(H_2O)_{1-4}]^-$

Geometries of $[HS_2O_7(H_2O)_{1-4}]^-$ conformers, optimized at the SCS-MP2/aVTZ level, are shown in Figure 3. Their binding energies are in Table 3. For this cluster size, the conformers which are less than 3 kcal/mol higher in energy than the global minimum are reported.

For $[HS_2O_7(H_2O)_1]^-$, there are six conformers. In the lowest one (***b***w$_1$0), the water molecule does not bind to the O3-H6 moiety. Rather, an effective H-bonding network is formed through O5-H12-O11-H13-O8, while the intramolecular H-bonding H6-O10 is maintained. The intramolecular H-boning is maintained in conformers of this cluster size except ***b***w$_1$2 and ***b***w$_1$5, in which a water molecule slides in between H6 and O10.

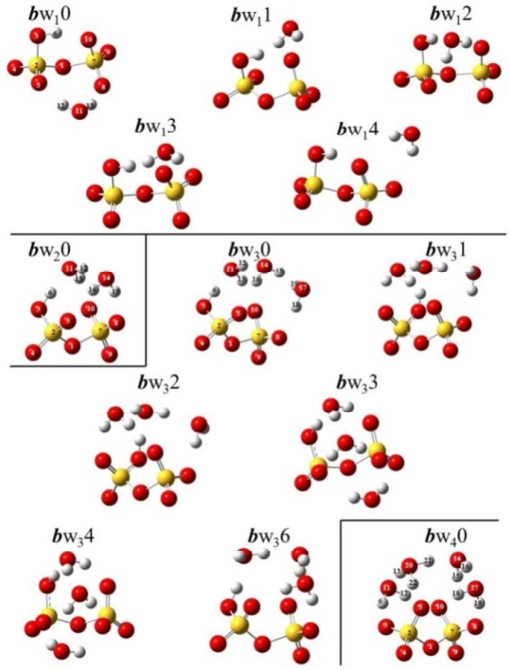

Figure 3. SCS-MP2/aVTZ optimized geometries of low energy conformers of $[HS_2O_7(H_2O)_{1\text{-}4}]^-$. Geometries of ***b***w$_1$5 and ***b***w$_2$5 (which are not shown here) are similar to those of ***b***w$_1$2 and ***b***w$_2$2, respectively; the major difference is in the degree of S7-O8-O9-O10 twisting.

For $[HS_2O_7(H_2O)_2]^-$, ***b***w$_2$0 is the only low energy conformer; the other conformers are at least 4.8 kcal/mol higher in M062X energy and are not reported here. In this lowest energy conformer, the intramolecular H-bonding is lifted as one water molecule slides in between H6 and O10 and the other two water molecules form an effective H-bonding network.

For $[HS_2O_7(H_2O)_3]^-$, seven conformers have similar energies in less than 1.1 kcal/mol. Except for ***b***w$_3$3 and ***b***w$_3$4, three water molecules tend to bind on the same side of the HS_2O_7 moiety. This would help to form a H-bonding network with all water molecules involved. Especially interesting is ***b***w$_3$2. This conformer does not show a deprotonation when optimized at the SCS-MP2/aVTZ level, while a deprotonated geometry with H6 closer to O11 appears when optimized with M062X/TZVP.

For $[HS_2O_7(H_2O)_4]^-$, ***a***w$_4$0 is a dominating conformer. Other conformers are at least 4.3 kcal/mol higher in M062X energy and thus are not reported here. In this conformer, all four water molecules bind on the same side of the $HS_2O_7^-$ moiety and form an effective H-bonding network. The deprotonation is clear in this conformer.

Table 3. Internal binding energies and Gibbs free energy changes of low energy conformers of $[HS_2O_7(H_2O)_{1\text{-}4}]^-$, optimized at the SCS-MP2/aVTZ level.[a]

		Binding energy	
		$-\Delta E_e(-\Delta E_0)$	$-\Delta G_{100K}$
$[HS_2O_7(H_2O)_1]^-$	***b***w$_1$0	11.4(9.20)	6.77
	bw$_1$1	10.6(8.11)	5.59
	bw$_1$2	10.7(7.99)	5.41
	bw$_1$3	9.86(7.78)	5.43
	bw$_1$4	9.70(7.59)	5.24
	bw$_1$5	9.74(7.07)	4.52
$[HS_2O_7(H_2O)_2]^-$	***b***w$_2$0	25.8(20.2)	14.9
$[HS_2O_7(H_2O)_3]^-$	***b***w$_3$0	36.5(28.7)	20.9
	bw$_3$1	35.5(28.1)	20.2
	bw$_3$2 [c]	35.0(28.0)	20.1
	bw$_3$3	35.3(28.0)	20.3
	bw$_3$4	35.8(27.9)	20.0
	bw$_3$5	34.9(27.6)	19.7
	bw$_3$6	35.5(27.6)	19.8
$[HS_2O_7(H_2O)_4]^-$	***b***w$_4$0 [b]	48.5(37.8)	27.2

[a]Refer to footnote of Table 2. [b]deprotonated geometry, [c] near deprotonated geometry

4. Discussion

4-1. Variation of geometries upon clustering with water

One of the most noteworthy findings in the cluster geometry is that the deprotonation of $H_2S_2O_7$ requires only two water molecules. This is the fewest number of water molecules that can induce the deprotonation in hydrated clusters of a monomer of strong Brönsted-Lowry acid reported so far. In the case of hydrated clusters of a dimer, H_2SO_4 dimer would be dissociated by two water molecules.[18]

The smaller number of water molecules for deprotonation must reflect the super acidic nature of $H_2S_2O_7$. Otto and Steudel calculated ΔG values for the gas phase deprotonation and used them to judge that acidities of $H_2S_2O_7$ and most other sulfur oxoacids are much stronger than H_2SO_4.[42] Abedi and Farrakhpour calculated ΔG for the deprotonation in the aqueous phase as well as in the gas phase and estimated pK_a values of sulfur oxoacids.[43] They showed that pK_{a1} of $H_2S_2O_7$ is lower than that of H_2SO_4 by at least 7. When pK_{a1} of other strong acids were included in the analysis, pK_{a1} of $H_2S_2O_7$ is lower than that of H_2SO_4 by about 4. Considering that pK_a of $HClO_4$ (reported to be -7 to -10 depending on references) is lower than pK_{a1} of H_2SO_4 (reported to be -4 to -10 depending on references) by smaller difference, $H_2S_2O_7$ is believed to be stronger than $HClO_4$. The number of water molecules for the deprotonation of these strong acids is consistent with their acid strength. The small number of water molecules for the deprotonation of $H_2S_2O_7$ may be possible owing to easy formation of H-bonding network with only two water molecules; the structure of $H_2S_2O_7$ has a flexible S-O-S frame across which two O-H bonds are positioned. This condition is also fulfilled in the deprotonated geometry of $(H_2SO_4)_2(H_2O)_2$.[18]

Another interesting finding is that deprotonation occurs in $HS_2O_7^-$ with only four water molecules. This is somewhat surprising since anions of Brönsted-Lowry acid are usually weak acids as the negative charge makes the second deprotonation very difficult. In Abedi and Farrokhpour's work[43], pK_{a2} of $H_2S_2O_7$ was estimated to be lower than that of H_2SO_4 by at least 3. Therefore, $HS_2O_7^-$ can be considered to be fairly strong.

Attention needs be paid to not only the deprotonation tendency but also other geometric variations upon addition of water molecules. For this purpose, we show Figure 4 to keep track of selected bond orders, sum of charges of certain moieties, etc. Especially, the behaviors of S7-O8-O9-O10 moiety along the series of water addition

have been our concern.

As the number of added water molecules increases in $H_2S_2O_7(H_2O)_n$, several geometrical parameters of the acid moiety become closer to those of $HS_2O_7^-$. O1-S7 bond weakens and $S(7)O_3$ moiety becomes more flat and negative. The decomposition $H_2S_2O_7 \rightarrow H_2SO_4 + SO_3$ appears close. However, the geometrical parameters of the acid unit in $H_2S_2O_7(H_2O)_n$ do not go beyond those of $HS_2O_7^-$ in favor of SO_3 decomposition; the O1-S7 bond order and the $S(7)O_3$ dihedral angle are still higher than those of HSO_4^-, even for $n \geq 3$. This implies that the decomposition would never occur until fully ionized HSO_4^- is formed.

Our next attention is the competition between the 2nd deprotonation and the O1-S7 dissociation. As water molecules are added in $HS_2O_7^-$, the deprotonation tendency increases. However, the O1-S7 bond strengthens, and the torsional angle of $S(7)O_3$ increases. Therefore, the SO_3 decomposition does not occur until the 2nd deprotonation occurs. In fact, the decomposition $H_2S_2O_7 \rightarrow H_2SO_4 + SO_3$ is endothermic and therefore hardly occurs at low temperatures. In contrast, our results suggest that the 1st and 2nd deprotonations occur readily at low temperatures. However, this situation should not be applied to the chemistry of oleum whose environment is very different.

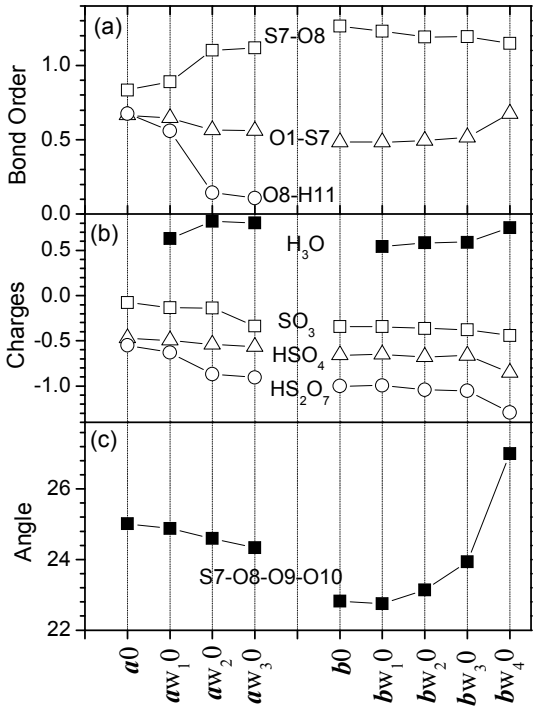

Figure 4. Variation of selected geometrical parameters; (a) Wiberg bond orders, (b) sum of NBO atomic charges, (c) dihedral angle of S7-O8-O9-O10. For charges, HSO_4 means the sum of atomic charges of H6, S2, O3, O4, O5; SO_3 means the sum of atomic charges of S7, O8, O9, O10; HS_2O_7 means the sum of charges of S1 through O10; H_3O means the sum of charges of H11, O12, H13, H14 for $[H_2S_2O_7(H_2O)_n]$ or H6, O11, H12, H13 for $[HS_2O_7(H_2O)_n]$.

4-2. Vibrational spectra

The M062X vibational spectra of the lowest energy conformers of $H_2S_2O_7(H_2O)_{0\text{-}3}$ and $[HS_2O_7(H_2O)_{0\text{-}4}]^-$ are shown in Figure 5. To facilitate the following discussion, we show only the low frequency region of the Raman spectra and the high frequency region of the IR spectra.

All vibrational peaks at higher than 2000 cm^{-1} correspond to O-H stretching modes. We classify them into A, B, C, D groups according to the kinds of O-H groups in motion and show them in Table 4. The total number of O-H stretching modes in each cluster is

2n+2 for $H_2S_2O_7(H_2O)_n$ and 2n+1 for $[HS_2O_7(H_2O)_n]^-$. The A and B groups are classified by the O-H stretching modes of unhydrated and hydrated acid O-H bonds, respectively. The modes of group A show large amplitudes of acid O-H stretchings and appear in frequency region between 3100 and 3430 cm^{-1}. When the acid O-H is bonded to a single water, the peaks shift to the region between 2020 and 2180 cm^{-1} with most intense IR activities. They involve an O-H···O antisymmetric stretching between an acid hydroxide and a water oxygen.

The C and D groups are classified by the OH-stretching modes of water and hydronium moiety. The modes of group C are found in the frequency region between 3160 and 3720 cm^{-1} with low IR intensities. The frequency values of group C are comparable to the experimental average value (3700 cm^{-1}) of free water molecule.[67] When no deprotonation occurs, there should be 2n modes of group C with or without H-bond interaction; this holds true for ***a***$w_1$0, ***b***$w_1$0, ***b***$w_2$0 and ***b***$w_3$0. But for the deprotonated conformers, ***a***$w_2$0, ***a***$w_3$0 and ***b***$w_4$0, there are the 2n-2 modes of group C. Instead, three O-H stretching modes (group D) of hydronium moiety (H_3O^+) in which the charged H-bonds interact strongly with water or acid moiety show up in the region between 2100 and 2820 cm^{-1} with enhanced IR activities as shown in Figure 5. The frequency region and the atomic motion of group D modes are very similar to a stretching vibration in the eigen structure of H_3O^+.[68-72] Therefore, The appearance of the group D peaks could identify the deprotonation of acid as shown for conformers ***a***$w_2$0, ***a***$w_3$0 and ***b***$w_4$0 (Figure 5).

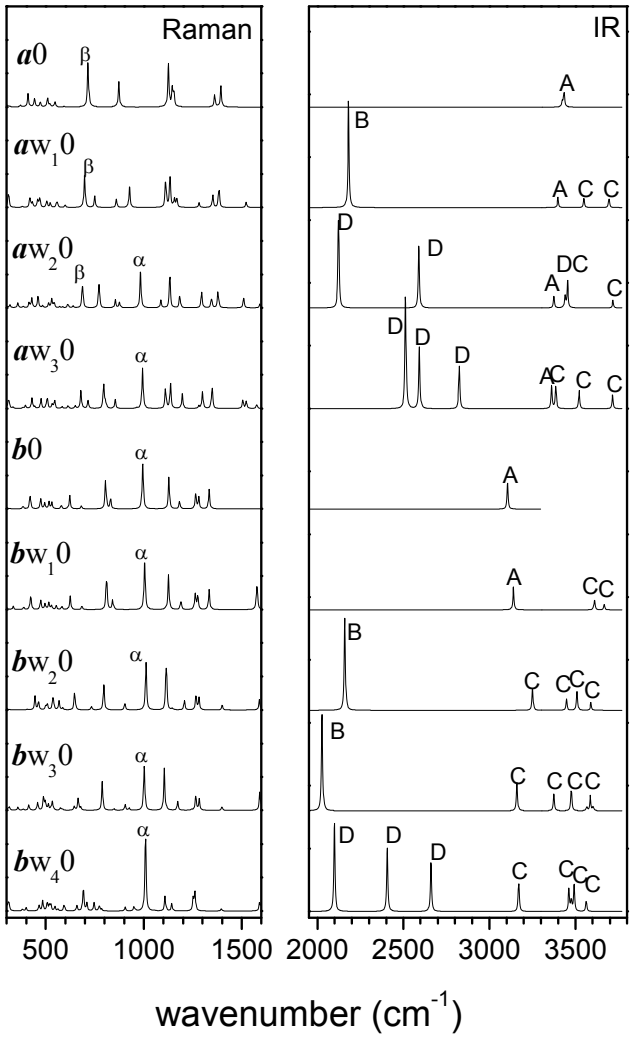

Figure 5. M062X Raman (left plots) and IR (right plots) spectra of the lowest energy conformers of $H_2S_2O_7(H_2O)_{0\text{-}3}$ and $[HS_2O_7(H_2O)_{0\text{-}4}]^-$. The frequency scale factor is 0.943. The vertical axis denotes the intensity in arbitrary unit. For the peak labels, refer to the footnote of Table 4.

Table 4. M062X OH stretching frequencies (cm^{-1}) classified into four groups

	Group A [a] [Group B][b]	Group C [c] [Group D][d]
$\boldsymbol{a}_0$	3423,3434	
$\boldsymbol{a}w_10$	3398 [2181]	3549,3694
$\boldsymbol{a}w_20$	3375	3454,3718 [2123,2590,3439]
$\boldsymbol{a}w_30$	3361	3385,3521,3715,3727 [2512,2592,2825]
$\boldsymbol{b}0$	3105	
$\boldsymbol{b}w_10$	3139	3610,3668
$\boldsymbol{b}w_20$	[2158]	3249,3447,3509 3590
$\boldsymbol{b}w_30$	[2026]	3161,3375,3477 3566,3586,3603
$\boldsymbol{b}w_40$		3170,3461,3463 3476,3492,3562 [2098,2406,2660]

[a]O-H stretchings of acid. [b]O-H--O antisymmetric stretching in between acid O-H and water. [c]O-H stretchings of water(s). [d]O-H stretchings of H_3O^+ moiety.

The vibrational spectra at low frequency region need be discussed with different viewpoints. With these low frequency spectra, many researchers have investigated Raman and IR characteristics of oleum,[47-51] as the high frequency spectra showed only unresolvable broad bands. As vibrational spectra of oleum in low frequency region consist of many closely-spaced peaks, contributed by major constituents H_2SO_4, SO_3, and $H_2S_2O_7$ and possible minor constituents of their products, the peak assignments have been ambiguous and controversial. Walafen measured the density and electrical conductivity of oleum solution at various SO_3 compositions.[49] They also obtained the Raman spectra of oleum solution and nitrated molten salt ($NO_2HS_2O_7$). Their elaborated analysis eliminated wrong peak assignment made in older publications and provided the range of SO_3 compositions for the distribution of major constituents: H_2SO_4, $H_2S_2O_7$,

SO_3, $H_2S_3O_{10}$, S_3O_9.

In their reported experimental Raman spectra of oleum, two intense polarized peaks were considered to be from $H_2S_2O_7$; a peak at 324 cm^{-1} was assigned to a deformation of S-O-S and a peak at 733 cm^{-1} was assigned to a symmetric stretching of S-O-S. However, no strong peak appears in the calculated Raman spectra in the region between 300 and 500 cm^{-1}. The experimental peak at 733 cm^{-1} is close to the peak 715 cm^{-1} for ***a***0 in the calculated Raman spectra. This peak in the calculation, labelled with β in Figure 5, is in fact S-O-S deformation with the depolarization ratio of 0.02.

Assignment for $HS_2O_7^-$ peaks in Walafen's Raman work was aided by the spectrum of nitrated molten salt, where an intense polarized peak was found at 1076 cm^{-1}. It is likely that this peak is a symmetric stretching of the SO_3 unit, which appears at 995 cm^{-1} in the calculated spectrum of ***b***0, labelled with α in Figure 5, this peak has the depolarization ratio of 0.01. This mode must be little affected by the surrounding since it appears in all $HS_2O_7^-$ clusters and ***a***$w_2$0 and ***a***$w_3$0 with little variations in frequency and intensity. However, this peak did not show up in the experimental Raman spectrum of oleum at the expected SO_3 compositions for disulfuric acid formation. Therefore, formation of $HS_2O_7^-$ as well as other ionic species as a major constituent of oleum is ruled out.

5. Concluding Remarks

In this paper, using DFT and ab initio theory, we studied hydrated clusters of $H_2S_2O_7$ and its anion $HS_2O_7^-$. We found that only two water molecules are needed to induce the first deprotonation of $H_2S_2O_7$. This is the fewest number of water molecules reported so far for water clusters of Brönsted-Lowry acids, and it reflects the super acidic nature of $H_2S_2O_7$. Even its deprotonated species $HS_2O_7^-$ requires only four water molecules for the second deprotonation. The deprotonation is convinced by observation of changes in vibrational spectra; specific three O-H stretching modes of hydrated hydronium moiety (H_3O^+) appear from the 3400 cm^{-1} to the 2700 cm^{-1} region with enhanced IR activity. The fewest number of water molecules for deprotonation would be possible since the flexible structure of $H_2S_2O_7$ allows a formation of an effective H-bonding network with only two

water molecules.

We also have looked into a possibility of decomposition $H_2S_2O_7 \rightarrow H_2SO_4 + SO_3$, which is a major reaction in oleum chemistry. As the number of water molecules in $H_2S_2O_7$ increases, not only the deprotonation tendency increases but also the S-O bond weakens. However, the decomposition leading to SO_3 formation does not occur until the 2nd deprotonation is completed as the addition of water molecules to $HS_2O_7^-$ strengthens the S-O bond.

Acknowledgements

This work was done during sabbatical research of SK Kim in the laboratory of KS Kim. We acknowledge the supported from NRF (National Honor Scientist Program: 2010-0020414) and KISTI (KSC-2014-C3-019, KSC-2014-C3-020)**.**

References

1 K. R. Leopold, *Annu. Rev. Phys. Chem.*, 2011, **62**, 327.

2 D. J. Miller and J. M. Lisy, *J. Am. Chem. Soc.*, 2008, **130**, 15393.

3 S. Karthikeyan, J. N. Singh, M. Park, R. Kumar and K. S. Kim, *J. Chem. Phys*., 2008, **128**, 244304.

4 S. J. Singh, A. C. Olleta, A. Kumar, M. Park, H. B. Yi, I. Bandyopadhyay, H. M. Lee, P. Tarakeshwar and K. S. Kim, *Theor. Chem. Acc*., 2006, **115**, 127.

5 H. M. Lee, P. Tarakeshwar, J. W. Park, M. R. Kolaski, Y. J. Yoon, H.-B. Yi, W. Y. Kim and K. S. Kim, *J. Phys. Chem. A*, 2004, **108,** 2949.

6 A. Laaksonen, *J. Chem. Phys.*, 2001, **114**, 3120.

7 M. Kolaski, H. M. Lee, C. Pak and K. S. Kim, *J. Am. Chem. Soc*., 2008, **130**, 103.

8 J. Kim, H. M. Lee, S. B. Suh, D. Majumdar and K. S. Kim, *J. Chem. Phys*., 2000, **113**, 5259.

9 A. Gutberlet, G. Schwaab, O. Birer, M. Masia, A. Kaczmarek, H. Forbert, M. Havenith and D. Marx, *Science,* 2009, **324**, 1545.

10 S. D. Flynn, D. Skvortsov, A. M. Morrison, T. Liang, M. Y. Choi, G. E. Douberly and A. F. Vilesov, *J. Phys. Chem. Lett.*, 2010, **1**, 2233.

11 D. Skvortsov, S. J. Lee, M. Y. Choi and A. F. Vilesov, *J. Phys. Chem. A*, 2009, **113**, 7360.

12 R. Iftimie, V. Thomas, S. Plessis, P. Marchand and P. Ayotte, *J. Am. Chem. Soc.*, 2008, **130**, 5901.

13 M. Kolaski, A. Zakharenko, S. Karthikeyan and K. S. Kim, *J. Chem. Theor. Comput.*, 2011, **7**, 3447;

14 G. Sedo, J. L. Doran and K. R. Leopold, *J. Phys. Chem. A*, 2009, **113**, 11301.

15 J. J. Panek and S. Berski, *Chem. Phys. Lett.*, 2008, **467**, 41.

16 W. H. Robertson and M. A. Jonhson, *Annu. Rev. Phys. Chem.*, 2003, **54**, 173.

17 B. Temelso, T. E. Morrell, R. M. Shields, M. A. Allodi, E. K. Wood, K. N. Kirschner, T. C. Castonguay, K. A. Archer and G. C. Shields, *J. Phys. Chem. A*, 2012, **116**, 2209.

18 B. Temelso, T. N. Phan and G. C. Shields, *J. Phys. Chem. A*, 2012, **116**, 9745.

19 M. Phonyiem, S. Chaiwongwattana, C. Laongam and K. Sagarik, *Phys. Chem. Chem. Phys.*, 2011, **13**, 10923.

20 R. Bianco, S. Wang and J. T. Hynes, *Adv. Quant. Chem.*, 2008, **55**, 387.

21 T. Kurtén, M. R. Sundberg, H. Vehkamaki, M. Noppel, J. Blomqvist, M. Kulmala, *J. Phys. Chem. A*, 2006, **110**, 7178.

22 D. L. Fiacco, S. W. Hunt and K. R. Leopold, *J. Am. Chem. Soc.*, 2002, **124**, 4504.

23 S. Karthikeyan, J. N. Singh and K. S. Kim, *J. Phys. Chem. A*, 2008, **112**, 6527.

24 A. Kumar, M. Park, J. Y. Huh, H. M. Lee and K. S. Kim, *J. Phys. Chem. A*, 2006, **110**, 12484.

25 A. C. Olleta, H. M. Lee and K. S. Kim, *J. Chem. Phys.*, 2007,**126**, 144311.

26 N. J. Singh, H.-B. Yi, S. K. Min, M. Park and K. S. Kim, *J. Phys. Chem. B*, 2006, **110**, 3808.

27 A. C. Olleta, H. M. Lee and K. S. Kim, *J. Chem. Phys.*, 2006, **124**, 024321.

28 A. R. Conrad, N. H. Teumelsan, P. E. Wang and M. J. Tubergen, *J. Phys. Chem. A*, 2010, **114**, 336.

29 A. Kumar, M. Kolaski and K. S. Kim, *J. Chem. Phys.*, 2008, **128**, 034304.

30 J. L. Alonso, E. J. Cocinero, A. Lesarri, M. E. Sanz and J. C. Lopez, *Angew. Chem. Int. Ed.*, 2006, **45**, 3471.

31 E. G. Diken, J. M. Headrick and M. A. Johnson, *J. Chem. Phys.*, 2005, **122**, 224317.

32 Y.-P. Zhu, Y.-R. Liu, T. Huang, S. Jiang, K.-M. Xu, H. Wen, W.-J. Zhang and W. Huang, *J. Phys. Chem. A*, 2014, **118**, 7959.

33 S. Odde, B. J. Mhin, S. Lee, H. M. Lee and K. S. Kim, *J. Chem. Phys*., 2004, **120**, 9524

34 S. Re, Y. Osamura, Y. Suzuki and H. F. Schaefer III, *J. Chem. Phys*., 1998, **109**, 973.

35 Z.-Z. Xie, Y.-S. Ong and J.-L. Kuo, *Chem. Phys. Lett.*, 2008, **453**. 13.

36 S. Odde, B. J. Mhin, K. H. Lee, H. M. Lee, P. Tarakeshwar and K. S. Kim, *J. Phys. Chem. A*, 2006, **110**, 7918.

37 J.-L. Kuo and M. L. Klein, *J. Chem. Phys.*, 2004, **120**, 4690.

38 A. A. Natsheh, A. B. Nadykto, K. V. Mikkelsen, F. Yu and J. J. Ruuskanen, *J. Phys. Chem. A*, 2004, **108**, 8914.

39 S. Re, Y. Osamura and K. Morokuma, *J. Phys. Chem. A*, 1999, **103**, 3535.

40 H. Arstila, K. Laasonen and A. Laaksonen, *J. Chem. Phys.*, 1998, **108**, 1031.

41 K. H. Weber and T.-M. Tao, *J. Phys. Chem. A.*, 2001, **105**, 1208.

42 A. Otto and R. Steudel, *Eur. J. Inorg. Chem*., 2001, 3047.

43 M. Abedi and H. Farrokhpour, *Dalton Trans*., 2013, **42**, 5566.

44 NIST Chemistry WebBook, http://webbook.nist.gov/chemistry/

45 J. R. Brayford and P. A. H. Wyatt, *Trans. Faraday Soc.*, 1956, **52**, 642.

46 B. Dacre and P. A. H. Wyatt, *Trans. Faraday Soc.*, 1961, **57**, 1281.

47 D. J. Millen, *J. Chem. Soc*., 1950, 2589.

48 G. E. Walrafen and T. F. Young, *Trans. Faraday Soc.*, 1960, **56**, 1419.

49 G. E. Walrafen, *J. Chem. Phys*., 1964, **40**, 2326.

50 R. J. Gillespie and E. A. Robinson, *Can. J. Chem*., 1962, **40**, 658.

51 P. A. Giguère and R. Savoie, *Can. J. Chem*., 1960, **38**, 2467.

52 M. Abedi, H. Farrokhpour, S. Farnia and A. N. Chermahni, *J. Mol. Struct.*, 2015, **1093**, 125.

53 D. Young, *Computational Chemistry: A Practical Guide for Applying Techniques to*

Real World Problems, Wiley-Interscience, 2001(Appendix A. A.1.6, pg 330, SPARTAN).

54 Y. Zhao, N. E. Schultz and D. G. Truhlar, *J. Chem. Theo. Comp.*, 2006, **2**, 364.

55 A. Schaefer, C. Huber and R. Ahlrichs, *J. Chem. Phys.*, 1994, **100**, 5829.

56 A. Hellweg, S. A. Grün and C. Hättig, *Phys. Chem. Chem. Phys*., 2008,**10**, 4119.

57 Weigend, M. Häser, H. Patzelt and R. Ahlrichs, *Chem. Phys. Lett.*,1998, **294**, 143.

58 Y. Cho, W. J. Cho, I. S. Youn, G. Lee, N. J. Singh and K. S. Kim, *Acc. Chem. Res*., 2014, **47**, 3321.

59 A. E. Reed, R. B.Weinstock and F. Weinhold, *J. Chem. Phys*., 1985, **83**, 735.

60 K. Wiberg, *Tetrahedron*, 1968, **24**, 1083.

61 M. J. Frisch, G. W. Trucks, H. B. Schlegel, G. E. Scuseria, M. A. Robb, J. R. Cheeseman, G. Scalmani, V. Barone, B.Mennucci, G.A. Petersson, H. Nakatsuji, M. Caricato, X. Li, H. P. Hratchian, A.F. Izmaylov, J. Bloino, G. Zheng, J. L. Sonnenberg, M. Hada, M. Ehara, K. Toyota, R. Fukuda, J. Hasegawa, M. Ishida, T. Nakajima,Y. Honda, O. Kitao, H. Nakai, T. Vreven, J. A. Montgomery, Jr., J. E. Peralta, F. Ogliaro, M. Bearpark, J. J. Heyd, E. Brothers, K. N. Kudin, V. N. Staroverov, T. Keith, R. Kobayashi, J. Normand,K. Raghavachari, A. Rendell, J. C. Burant, S. S. Iyengar, J.Tomasi, M. Cossi, N. Rega, J. M. Millam, M. Klene, J. E. Knox, J.B. Cross, V. Bakken, C. Adamo, J. Jaramillo, R. Gomperts, R. E.Stratmann, O. Yazyev, A. J. Austin, R. Cammi, C. Pomelli, J. W.Ochterski, R. L. Martin, K. Morokuma, V. G. Zakrzewski, G. A.Voth, P. Salvador, J. J. Dannenberg, S. Dapprich, A. D. Daniels, O. Farkas, J. B. Foresman, J. V. Ortiz, J. Cioslowski and D. J. Fox, *2010 Gaussian 09, RevisionB.01*, Gaussian, Inc.

62 F. Furche, R. Ahlrichs, C. Hättig, W. Klopper, M. Sierka and F. Weigend, *WIREs Comput. Mol. Sci.*, 2014, **4**, 91.

63 I. D. Brown and R. J. Gillespie, *Inorg. Chem*., 1971, **10**, 2319.

64 T. Helgaker, W. Klopper, H. Koch and J. Noga, *J. Chem. Phys.*, 1997, **106**, 9639.

65 S. K. Min, E. C. Lee, H. M. Lee, D. Y. Kim, D. Kim, K. S. Kim, *J. Comput. Chem.* 2007, **29**, 1208.

66 P. Hobza, J. Šponer, *J. Am. Chem. Soc.* 2002, **124**, 11802.

67. P. E. Fraley and K. N. Rao, *J. Mol. Spectrosc*., 1969, **29**, 348.

68 J.-W. Shin, N. I. Hammer, E. G. Diken, M. A. Johnson, R. S. Walters, T. D. Jaeger, M. A. Duncan, R. A. Christie and K. D. Jordan, *Science*, 2004, **304**, 1137.

69 M. Miyazaki. A. Fujii, T. Ebata and N. Mikami, *Science*, 2004, **304**, 1134.

70 J. M. Headrick, E. G. Diken, R. S. Walters, N. I. Hammer, R. A. Christie, J. Cui, E. M. Myshakin, M. A. Duncan, M. A. Johnson and K. D. Jordan, *Science*, 2005, **308**, 1765.

71 M. Park, I. Shin, N. J. Singh and K. S. Kim, *J. Phys. Chem. A*, 2007, **111**, 10692.

72 H.-C. Chang, C.-C. Wu and J.-L. Kuo, *Int. Rev. Phys. Chem.*, 2005, **24**, 553.